STRUCTURAL INTEGRITY DESIGN OF A COMPOSITE WING IN A TILTROTOR AIRCRAFT

Jaehoon Lim,[1,*] Taeseong Kim,[2] SangJoon Shin,[3] and Do-Hyung Kim[4]
[1,3] School of Mechanical and Aerospace Engineering, Seoul National University, Seoul, Republic of Korea
[2] Wind Energy Division, Risoe DTU, Roskilde, 4000, Denmark
[4] Korea Aerospace Research Institute, Daejeon, Republic of Korea
* Corresponding author (jake30@snu.ac.kr)

Keywords: *Stress/strain recovery, Whirl flutter, Optimization, Tiltrotor aircraft*

1 Introduction

Whirl flutter instability generally imposes a limit on cruise performance in a tiltrotor aircraft. Therefore, much research has been conducted to enhance its aeroelastic stability using numerical and experimental methods [1, 2]. And the active control algorithm employed by the actuation of the wing flaperon and the swashplate was examined for whirl flutter stability and robustness augmentation [3]. Recently, a design optimization framework for tiltrotor composite wings considering whirl flutter stability was developed [4]. And a tiltrotor whirl flutter stability analysis and optimization framework to enhance whirl flutter stability [5] was developed by the present authors. In this framework, pitch-flap coupling, wing vertical, chordwise bending stiffness, and torsional stiffness were determined to improve the tiltrotor whirl flutter stability. And then the wing configuration which satisfies the determined structural properties is suggested. Also the suggested wing should be structurally safe for a given flight condition. In this paper, a MATLAB-based 3-D stress/strain recovery module is developed to conduct the structural integrity analysis of the composite wing cross section.

2 Tiltrotor Whirl Flutter Stability Analysis and Optimization Framework

To enhance the aeroelastic stability of a tiltrotor aircraft, structural optimization framework was developed using a two-level optimization approach as shown in Figure 1. Maximization of the flutter speed was selected as an object for the upper-level optimization by changing the structural properties of the wing. XV-15 tiltrotor aircraft was selected as an object of the present analysis. Table 1 shows a brief summary of the aircraft used. For aeroelastic analysis, an existing in-house analysis model was used. The object of the lower-level optimization was to replace the structural properties used in the upper-level optimization with composite materials by adding design parameters, such as ply angles, layer thickness, spar positions, and etc. In order to analyze the composite wing cross-section, UM/VABS [6] was used. The results obtained from the upper-level optimization gave approximately 10% increase in terms of the flutter speed when using the unsteady aerodynamics model as shown in Table 2. And Table 3 shows the optimized prediction results for the structural stiffness to enhance whirl flutter stability.

At the lower-level optimization, two different design cases were obtained by changing the composite materials. In those cases, detailed results about the discrete orientation angles, integral number of plies, and the spar positions were obtained. Figure 2 shows a sketch of the cross-section of the wing with optimum design values for Case 1. The front spar was located at 0.29*c*, and the aft one was at 0.39*c*, respectively. A symmetric stack sequence was used for the spar cabs and the spars. The ply orientation angles, accordingly, were $[0_6]$, $[30_{17}/30_{27}/\text{-}90_{26}/30_{30}]_s$, and $[30_{22}/90_{22}/30_{22}/90_{22}]_s$ for the skin, spar cabs, and spars, respectively. In this case, E-glass was used in all regions. The result of Case 2 is illustrated in Figure 3. The front shear web was located at 0.28*c* and the rear one was at 0.35*c*, respectively. A symmetric stack sequence was used for the spar cabs and the spars. The ply orientation angles were $[0_7]$, $[30_5/30_{12}/45_{15}/\text{-}45_{24}]_s$, and $[\text{-}30_{25}/45_{25}/\text{-}30_{25}/45_{25}]_s$ for the skin, spar cabs, and spars, respectively. In this case, E-glass was used for the skin and the spars and T300/5280 Graphite/epoxy was used for the spar cabs.

3 Three-dimensional Stress/strain Recovery

To conduct the structural integrity analysis of the optimized composite wing cross section, a MATLAB-based 3-D stress/strain recovery module is developed as shown in Figure 4. Using the inverse form of the one-dimensional global beam constitutive relation, Eq. (1), the strain and curvatures are obtained at a wing station as a function of the internal forces and moments.

$$\begin{Bmatrix} \gamma_1 \\ \kappa_1 \\ \kappa_2 \\ \kappa_3 \end{Bmatrix} = \left[K\right]^{-1} \begin{Bmatrix} F_1 \\ M_1 \\ M_2 \\ M_3 \end{Bmatrix} \tag{1}$$

where [K] is the stiffness matrix from UM/VABS cross sectional analysis γ_1 is the axial strain, κ_1 is the elastic twist and κ_2 , κ_3 are two bending curvatures. The internal forces and moments at each blade station are predicted by CAMRAD II [7]. The strain and curvatures obtained at a wing station are multiplied to the strain influence matrix for each element obtained from UM/VABS 3D stress/strain recovery. In addition, a safety factor of 1.5 is considered. The maximum strain criterion is applied for each component in the resulting strain and it is compared with the allowable values for the local constituent material.

5. Results

The structural integrity analysis is conducted using the MATLAB based 3-D stress/strain recovery analysis module. The internal forces and moments at each blade station are predicted by CAMRAD II under the assumption of cruising at 330 knots, which is the maximum design speed of XV-15 aircraft.

The present semi-span aircraft CAMRAD II input consists of an airframe and two rotors. In this case, internal loads are not obtained by the load sensors directly. Thus the internal loads are estimated by the lift, drag, pitching moment, up and thrust predicted upon the rotors. Lift and drag on the wing are then assumed to distribute uniformly.

The flapwise bending moment is generated from the lift on the wing and the torque by the rotors. And the lead-lag bending moment is from the drag on the wing and the thrust by the rotors. The torsional moment is from the pitching moment at the trim condition. In this analysis, because of the limitation of the airframe model, it is assumed that the lift and drag on the wing will be constant along the spanwise direction. Table 4 shows the resulting internal forces and moments at each section. The present MATLAB based 3-D strain recovery module is used for Case 1 using the internal forces and moments. The material properties of E-glass considered in Case 1 are shown in Table 5. Tables 6 and 7 show the analysis results of the wing cross section for Case 1. The maximum shear strain occurs at the tip of the wing and it is 62.9 percent of the allowable strain of the material. Therefore the suggested wing is found to be structurally safe at the maximum design speed. The present MATLAB based 3-D strain recovery module will also be used for Case 2, which considers two different materials. In that case, since the maximum allowable strain values of T300/5280 Graphite/epoxy are lower than that of E-glass, a lower margin for the structural safety will be expected.

6 Conclusion

Recently, a structural optimization framework was developed by using a two-level approach for a composite wing design to increase whirl flutter speed by those authors. By this framework, two wing configurations satisfying the aeroelastically optimized structural properties are suggested. The suggested wing should be structurally safe for a given flight condition. Thus a MATLAB-based 3-D stress/strain recovery module is developed additionally to conduct the structural integrity analysis of the composite wing cross section. And the structural integrity analysis is conducted for Case 1 using the developed failure analysis module. As a result, the suggested wing is structurally safe at the maximum design speed.

The stress/strain recovery analysis will be conducted for Case 2. And considering several important factors such as the position of the elastic center and aerodynamic center, many different wing configurations which satisfy the aeroelastically optimized structural properties will be suggested. And then the strain recovery failure analysis will also be applied to the additionally suggested composite wing cross sections.

And because of the uniform lift distribution assumed along the wing span, the resulting internal forces and moments may not be accurate. Thus in the future CAMRAD II analysis, wing will be analyzed as one of the rotors, instead of an airframe. Therefore more realistic distribution for the lift and drag along the wing span will be considered.

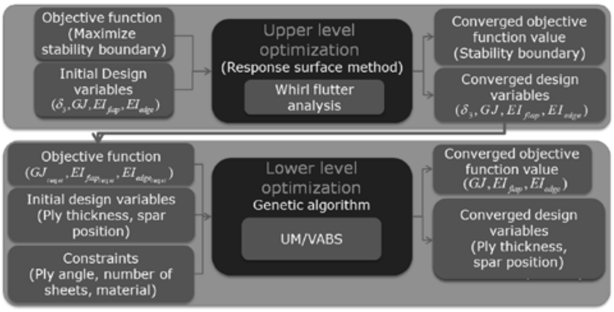

Fig. 1. Flowchart of the tiltrotor whirl flutter stability analysis and optimization framework

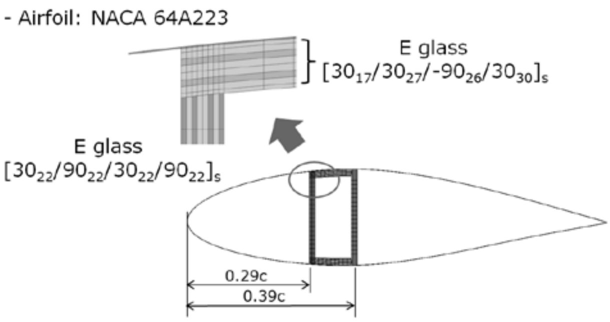

Fig. 2. A sketch of the cross-section of the composite sing (Case 1)

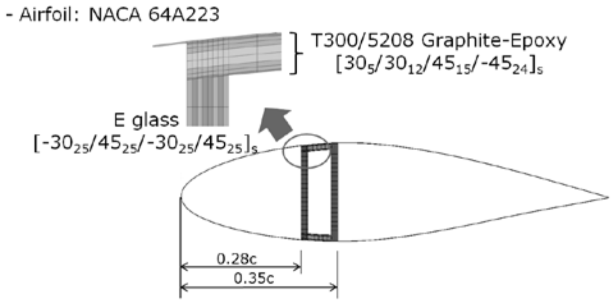

Fig. 3. A sketch of the cross-section of the composite wing (Case 2)

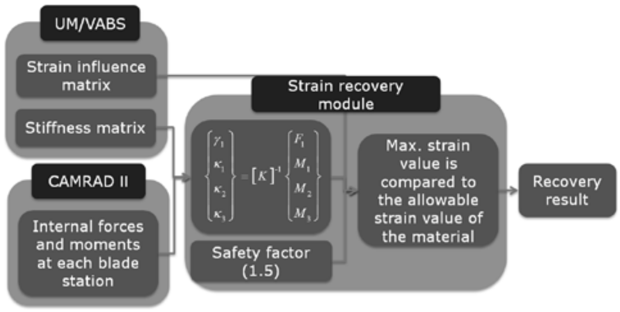

Fig. 4. Flowchart of the MATLAB-based 3-D stress/strain recovery module

Table 1. Properties of the XV-15 aircraft

Rotor system	
Number of blade, *N*	3
Radius, *R*	3.8 m
Lock number, γ	3.83
Solidity, σ	0.089
Wing	
Airfoil	NACA 64A223
Semispan, $y_{w_{tip}}$	4.88 m
Chord, c_w	1.57 m
Mast height, h_m	0.99 m

Table 2. Result for the whirl flutter speed [5]

	Baseline	Optimum	Difference (%)
Whirl flutter	330 knots	365 knots	Approx. 10

speed

Table 3. Results for the structural stiffness

	Target values(N-m^2)
EI_f	6.89×10^6
EI_e	1.87×10^7
GJ	2.21×10^6

Table 4. Internal forces and moments

Spanwise location (m)	Torsion (N-m)	Flapwise bending moment (N-m)	Lead-lag bending moment (N-m)
0	-24,195	-2,480	-16,239
0.61	-24,195	-15,890	-16,224
1.22	-24,195	-27,522	-15,640
1.83	-24,195	-37,376	-14,486
2.44	-24,195	-45,452	-12,763
3.05	-24,195	-51,750	-10,471
3.66	-24,195	-56,269	-7,609
4.27	-24,195	-59,011	-4,179
4.88	-24,195	-59,974	-179

Table 5. Material properties and maximum allowable strain values of E-glass 120

Material propertiy	
E_{11}	14,800 MPa
E_{22}	13,600 MPa
G_{12}	1,900 MPa
υ_{12}	0.19
Maximum strain values	
Longitudinal tensile	14,286 μ strain
Longitudinal compression	-14,286 μ strain
Transverse tensile	15,857 μ strain
Transverse compression	-15,857 μ strain
Shear	22,167 μ strain

Table 6. Maximum normal strain result

	Max. normal strain, (μ strain)	Spanwise location
Recovery result	2535.4 (17.8 % of allowable strain)	4.88 m

Table 7. Maximum shear strain result

	Max. shear strain, (μ strain)	Spanwise location
Recovery result	13,940 (62.9 % of allowable strain)	4.88 m

Acknowledgments

This work is supported by Defense Acquisition Program Administration and Agency for Defense Development in Republic of Korea under the contract UD100048JD.
This work was supported by the New and Renewable Energy Program of the Korea Institute of Energy Technology Evaluation and Planning (KETEP) grant funded by the Korea government Ministry of Knowledge Economy (No.20104010100490)

References

[1] Hall, Jr., W. E., "Prop-Rotor Stability at High Advance Ratios," *Journal of the American Helicopter Society*, Vol. 11, No. 2, April 1966.

[2] Acree, C. W., Peyran, Jr., R. J., and Johnson, W., "Rotor Design Options for Improving XV-15 Whirl-Flutter Stability Margins," NASA Technical Paper-2004-212262, March, 2004.

[3] Kvaternik, R. G., and Kohn, J. S., "An Experimental and Analytical Investigation of Proprotor Whirl Flutter," NASA Technical Paper-1047, Dec, 1977.

[4] Park, J-S., Jung, S., Lee, M., and Kim, J., "Design Optimization Framework for Tiltrotor Composite Wings Considering Whirl Flutter Stability," *Composites Part B: Engineering*, Vol. 41, No. 4 June, 2010, pp. 257-267.

[5] Kim, T., Lim, J., Lee, J., and Shin, S.-J., "Structural Design and Optimization of a Tiltrotor Aircraft to Enhance Whirl Flutter Stability," The International Powered Lift Conference, Philadelphia, PA, October 5-7, 2010.

[6] Palacios, R. and Cesnik, C. E. S., "Cross-Sectional Analysis of Non-Homogeneous Anisotropic Active Slender Structures," *AIAA Journal*, Vol. 43, No. 12, 2005, pp. 2624-2638.

[7] Johnson, W., "Technology Drivers in the Development of CAMRAD II," Proceedings of the AHS Aeromechanics Specialist Conference, AHS International, Alexandria, VA, 1994, pp 3.1-3.14.

[8] Shin, S.-J., "Design, Manufacturing and Testing of an Active Twist Rotor," M.S. Thesis, Massachusetts Institute of Technology, 1999.